

# Optical characterization of $\text{CuIn}_5\text{S}_8$ crystals by ellipsometry measurements



Mehmet Isik<sup>a,\*</sup>, Nizami Gasanly<sup>b,c</sup>

<sup>a</sup> Department of Electrical and Electronics Engineering, Atılım University, 06836 Ankara, Turkey

<sup>b</sup> Department of Physics, Middle East Technical University, 06800 Ankara, Turkey

<sup>c</sup> Virtual International Scientific Research Centre, Baku State University, 1148 Baku, Azerbaijan

## ARTICLE INFO

### Article history:

Received 29 May 2015

Received in revised form

28 October 2015

Accepted 25 November 2015

Available online 27 November 2015

### Keywords:

A. Semiconductors

A. Optical materials

D. Optical properties

## ABSTRACT

Optical properties of  $\text{CuIn}_5\text{S}_8$  crystals grown by Bridgman method were investigated by ellipsometry measurements. Spectral dependence of optical parameters; real and imaginary parts of the pseudodielectric function, pseudorefractive index, pseudoextinction coefficient, reflectivity and absorption coefficients were obtained from the analysis of ellipsometry experiments performed in the 1.2–6.2 eV spectral region. Analysis of spectral dependence of the absorption coefficient revealed the existence of direct band gap transitions with energy 1.53 eV. Wemple–DiDomenico and Spitzer–Fan models were used to find the oscillator energy, dispersion energy, zero-frequency refractive index and high-frequency dielectric constant values. Structural properties of the  $\text{CuIn}_5\text{S}_8$  crystals were investigated using X-ray diffraction and energy dispersive spectroscopy analysis.

© 2015 Elsevier Ltd. All rights reserved.

## 1. Introduction

The ternary semiconducting compound  $\text{CuIn}_5\text{S}_8$  has the same cubic spinel structure as  $\text{CdIn}_2\text{S}_4$  [1]. This crystal can be derived from the  $\text{CdIn}_2\text{S}_4$ , if the divalent cadmium cations are replaced by the univalent copper cations and trivalent indium cations, according to the following transformation:  $\text{CdIn}_2\text{S}_4 = > [\text{Cu}_{1/2}\text{In}_{1/2}]_2[\text{In}_2]_0 = > \text{Cu}_{1/2}\text{In}_{5/2}\text{S}_4 = > \text{CuIn}_5\text{S}_8$ . Thus, in the  $\text{CuIn}_5\text{S}_8$  crystal 1/5 of the indium cations have tetrahedral (t) and 4/5 of the indium cations have octahedral (o) coordination. The semiconductor compound  $\text{CuIn}_5\text{S}_8$  is the visible-light-active material with high-absorption coefficient, suitable band gap, good radiation stability, and easy conversion between n- and p-type carrier types which permit a variety of potentially low-cost homo- and hetero-junction [2,3].  $\text{CuIn}_5\text{S}_8$  crystal has been confirmed as material suitable for use in photoelectrochemical and conventional solar cells, high-frequency thin films convertors and infrared detectors [4,5].

The optical and electrical properties of  $\text{CuIn}_5\text{S}_8$  have been studied in Refs. [6–12]. The energy band gap for the direct optical transitions of  $\text{CuIn}_5\text{S}_8$  are found as 1.51 and 1.57 eV at 295 and 77 K, respectively [13]. Infrared reflection and Raman scattering spectra of  $\text{CuIn}_5\text{S}_8$  crystals have also been investigated and analyzed in Refs. [14–16]. Photoluminescence (PL) spectra of  $\text{CuIn}_5\text{S}_8$  crystals were obtained in the temperature range of 10–34 K [17].

The observed PL band centered at 1.44 eV was attributed to the radiative recombination of charge carriers from donor ( $E_d = 17$  meV) to acceptor ( $E_a = 193$  meV) states.

In this article, we investigate the optical properties of  $\text{CuIn}_5\text{S}_8$  crystals by means of ellipsometry measurements. The spectral dependence of real and imaginary parts of pseudodielectric function, pseudorefractive index and pseudoextinction coefficient are presented. The wavelength dependence of pseudorefractive index in the below band gap energy region was analyzed using Wemple–DiDomenico and Spitzer–Fan models to find oscillator energy, dispersion energy, zero-frequency refractive index, zero- and high-frequency dielectric constants. Moreover, the crystal structure and atomic composition of  $\text{CuIn}_5\text{S}_8$  crystals were investigated using X-ray diffraction and energy dispersive spectroscopy analysis.

## 2. Experimental details

$\text{CuIn}_5\text{S}_8$  semiconductor polycrystals were synthesized using high-purity elements taken in stoichiometric proportions. Copper (Fluka cat. no. 61140), indium (Fluka cat. no. 57077) and sulfur (Fluka cat. no. 84680) were of 99.999% purity. The single crystals were grown by the Bridgman method from resultant polycrystalline ingots in evacuated ( $10^{-5}$  Torr) silica tubes (10 mm in diameter and about 15 cm in length) with a tip at the bottom in our crystal growth laboratory. No seed crystal was used. After evacuation and sealing off, the tube was introduced into the upper zone of a vertical two-zone furnace. The temperatures in the upper

\* Corresponding author.

E-mail address: [mehmet.isik@atilim.edu.tr](mailto:mehmet.isik@atilim.edu.tr) (M. Isik).

and lower zones were about 1130 and 840 °C. The temperature gradient between the zones was 30 °C cm<sup>-1</sup>. After melt homogenization for 2 h, the tube was lowered through the gradient zone at a rate of 1.0 mm h<sup>-1</sup>. Then the tube was pulled to the cold zone at the same rate, and the grown crystal was homogenized at 840 °C for 50 h. After that, the temperature of the cold zone was lowered to 600 °C and then the furnace was shut off. The resulting ingot with 8.5 mm in diameter and about 35 mm and 9 g in length and mass, respectively, was air/moister stable. The final ingot exhibited monocrystalline nature. The samples selected for the measurements were taken from the middle part of the ingot.

The crystal structure properties were identified using X-ray diffraction (XRD) experiments. Measurements were performed using “Rigaku Miniflex” diffractometer with CuK $\alpha$  radiation ( $\lambda=0.154049$  nm). The scanning speed of the diffractometer was 0.02°/s. Experiments were accomplished in the diffraction angle ( $2\theta$ ) range of 10–90°. The ellipsometric measurements on the CuIn<sub>5</sub>S<sub>8</sub> single crystals were carried out at room temperature in the 1.2–6.2 eV spectral range using SOPRA GES-5E rotating polarizer ellipsometer. The incidence angle of the light beam was 70°. In order to carry out the ellipsometric measurements, the ingots were cut and the surfaces produced were ground and polished carefully according to optical techniques to have the highest optical quality. Before the spectroscopic ellipsometry measurements, the samples were mechanically polished with 0.5  $\mu$ m Al<sub>2</sub>O<sub>3</sub> powder, followed by chemical polishing with an alkaline solution, and finally rinsed with deionized water.

### 3. Results and discussion

Fig. 1 presents the energy dispersive spectrum of CuIn<sub>5</sub>S<sub>8</sub> crystal. The atomic composition ratio of the studied sample (Cu:In:S) was found as 6.7:37.9:55.4, respectively. XRD technique was used to obtain the structural parameters of the CuIn<sub>5</sub>S<sub>8</sub> spinel type crystals. The crystal system, Miller indices of the diffraction peaks and lattice parameters were evaluated using a least-squares computer program “TREOR90”.

Fig. 2 shows the X-ray diffractogram of CuIn<sub>5</sub>S<sub>8</sub>. The sharp diffraction peaks are the indication of the well crystallinity of the sample. The full-widths at half-maximum of peaks ranged from 0.2° to 0.5°. Miller indices ( $h k l$ ) are shown on the diffraction peaks. Moreover, the intensities of the observed and those of previously reported peaks are given in Table 1 [18,19]. The lattice parameter of the cubic unit cell of CuIn<sub>5</sub>S<sub>8</sub> crystals was found to be

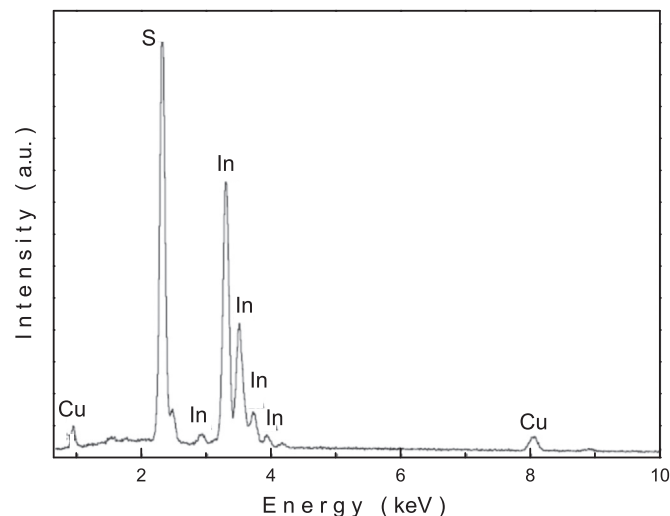


Fig. 1. Energy dispersive spectroscopic analysis of CuIn<sub>5</sub>S<sub>8</sub> crystal.

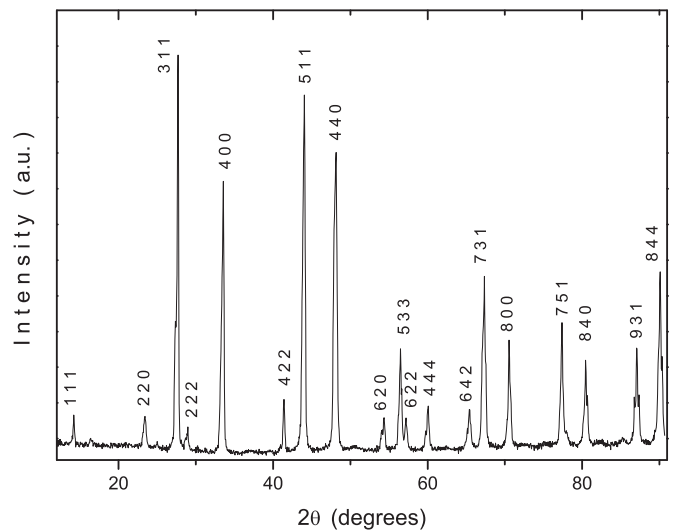


Fig. 2. X-ray powder diffraction pattern of CuIn<sub>5</sub>S<sub>8</sub>.

Table 1  
X-ray powder diffraction data for CuIn<sub>5</sub>S<sub>8</sub> crystals.

$h k l$	$I/I_0$ (Present work)	$I/I_0$ Ref. [18]	$I_{obs}$ Ref. [19]
1 1 1	8	20	–
2 2 0	9	25	w
3 1 1	100	100	vs
2 2 2	5	10	–
4 0 0	68	30	s
4 2 2	12	10	w
5 1 1	90	50	s
4 4 0	75	70	s
6 2 0	7	2	w
5 3 3	25	15	m
6 2 2	7	5	w
4 4 4	10	10	m
6 4 2	9	5	m
7 3 1	43	20	s
8 0 0	27	10	m
7 5 1	32	10	s
8 4 0	22	5	s
9 3 1	25	5	ms
8 4 4	45	2	s

w: weak, m: medium, vs: very strong, s: strong, ms: medium strong.

$a=1.0687$  nm. This parameter value is well correlates with that reported previously in Ref. [20].

Ellipsometry measurements were carried out on CuIn<sub>5</sub>S<sub>8</sub> crystals in the 1.2–6.2 eV range to get information about the spectral dependencies of optical parameters. The amplitude ratio ( $\Psi$ ) and phase shift ( $\Delta$ ) of the parallel and perpendicular components of the reflected light are taken as outcome of ellipsometry experiments. These two parameters are analyzed using air/sample optical model in which pseudodielectric function is found from the relation [21]

$$\langle \epsilon \rangle = \langle \epsilon_1 \rangle + i \langle \epsilon_2 \rangle = \sin^2(\phi) \left[ 1 + \left( \frac{1-\rho}{1+\rho} \right)^2 \tan^2(\phi) \right], \quad (1)$$

where  $\phi$  is the angle of incidence and  $\rho$  is the complex reflectance ratio of the polarized light. The “pseudo” word is added in front of the designation of the optical parameters obtained from the measured values of  $\Psi$  and  $\Delta$  [21]. Fig. 3 shows the spectra of real and imaginary parts of the pseudodielectric function. The spectrum of  $\langle \epsilon_2 \rangle$  exhibits one peak around 4.1 eV which can be associated with strong absorption of photon energy at the

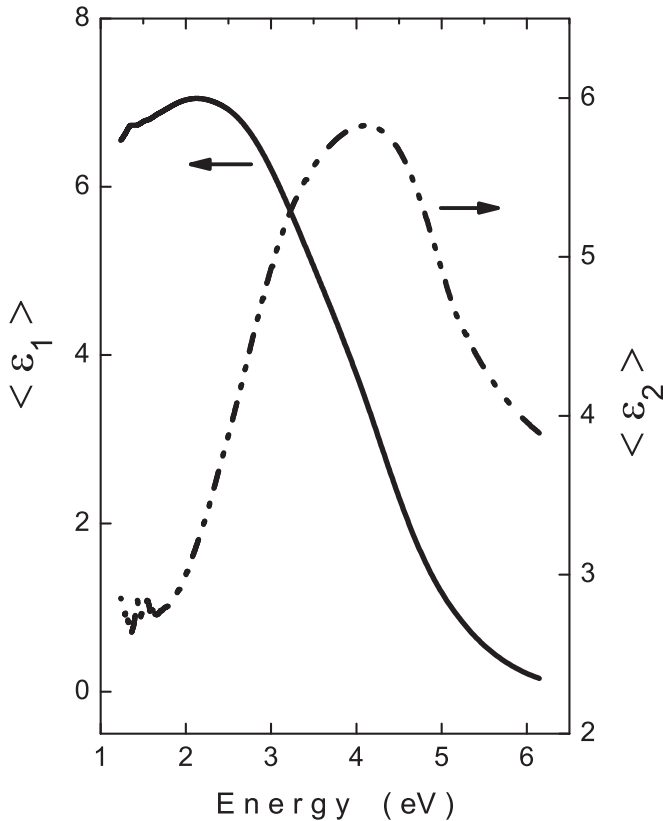


**Fig. 3.** Spectral dependencies of the pseudodielectric functions of  $\text{CuIn}_5\text{S}_8$ . Solid and dot-dashed curves represent the real and imaginary part of spectra, respectively.

corresponding interband transition [22–24]. Moreover, it is observed from the same spectrum that  $\epsilon_2$  value is not equal to zero below band gap energy ( $E_g = 1.53$  eV). This situation disobeying the theoretical fact can be the result of intrinsic contributions (alloy disorder) and deviation from stoichiometry. Similar absorption tails were also reported previously in the results of ellipsometry analysis of  $\text{CuIn}_5\text{Se}_8$  and  $\text{CuGa}_5\text{Se}_8$  [25] and  $\text{CuAl}_x\text{In}_{1-x}\text{Se}_2$  [26].

The optical parameters, pseudorefractive index and pseudoextinction coefficient have been calculated using well known equations relating these parameters to components of pseudodielectric function [27]. Fig. 4 shows the spectral dependences of mentioned optical parameters. Pseudorefractive index slightly increases with energy from 2.63 to 2.74 in the region of 1.2–2.4 eV. For  $h\nu > 2.5$  eV region, pseudorefractive index shows a sharp decrease with energy. The spectrum of the  $n$  presented in Fig. 4 exhibits the pseudorefractive index value as 2.67 corresponding to the band gap energy. The refractive index obtained from transmission and reflection measurements on  $\text{CuIn}_5\text{S}_8$  thin films increased from 2.50 to 2.65 with rising of photon energy from 0.73 to 1.55 eV [9]. Besides, we compare the extinction coefficient values with the results of study reported in the literature [9]. For this purpose, we examine the extinction coefficients corresponding to  $\lambda = 600$  nm ( $E = 2.07$  eV), which is the only common wavelength with the result of other work. The extinction coefficient value of our crystal  $\text{CuIn}_5\text{S}_8$  has been found as 0.57 from the ellipsometry measurements. The extinction coefficient for the same wavelength obtained in previous work from transmission and reflection measurements on  $\text{CuIn}_5\text{S}_8$  thin films varied between 0.10 and 0.80 for the substrate temperatures from 30 to 200 °C.

The refractive index ( $n$ ) of semiconductors typically increases as band gap energy  $E_g$  decreases. There are various empirical and semi-empirical relations and expressions that relate  $n$  to  $E_g$  [27]. In

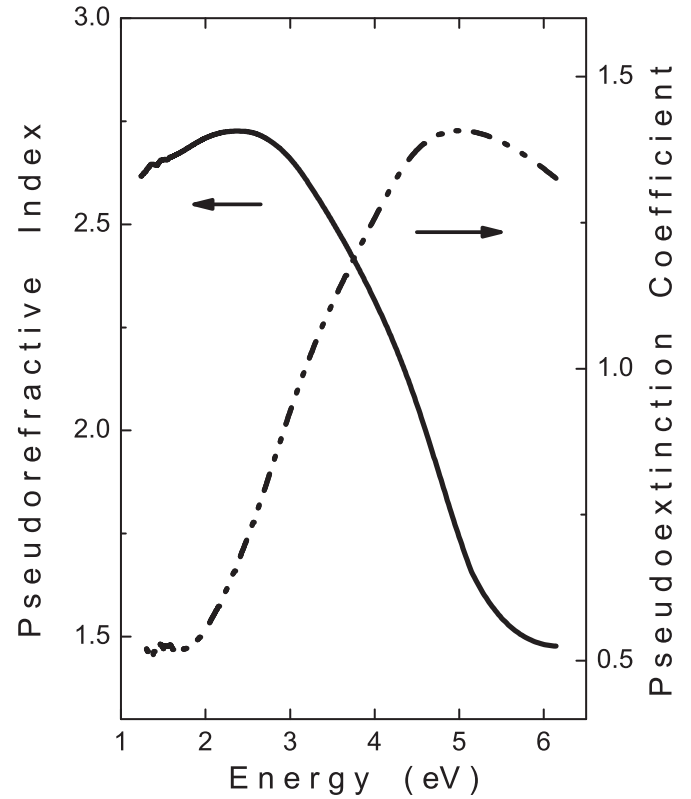


**Fig. 4.** Spectral dependencies of the pseudorefractive index and pseudoextinction coefficient of  $\text{CuIn}_5\text{S}_8$ . Solid and dot-dashed curves represent the pseudorefractive index and pseudoextinction coefficient spectra, respectively.

Moss relation,  $n$  and  $E_g$  are related by the expression

$$n^4 E_g = K \quad (2)$$

where  $K$  is a constant which is approximately equal to 95 eV. By using Moss relation, we calculated the refractive index of  $\text{CuIn}_5\text{S}_8$  crystal as 2.81. The magnitudes of refractive indices, determined by relation (2) from experiments on  $\text{CuIn}_5\text{S}_8$  thin films, were ranged from 2.65 to 2.80, dependent on substrate temperatures [9].

Reflectivity ( $R$ ) was computed using the refractive index  $n$  and absorption index  $k$  values by means of the following relation [27]

$$R = \frac{(n-1)^2 + k^2}{(n+1)^2 + k^2} \quad (3)$$

The absorption coefficient ( $\alpha$ ) is connected to the absorption index  $k$  by relationship  $\alpha = 4\pi k/\lambda$ , where  $\lambda$  is the wavelength. The calculated spectral dependencies of the reflectivity and absorption coefficients of  $\text{CuIn}_5\text{S}_8$  crystals are presented in Fig. 5.

Band gap energy  $E_g$  of the crystal can be obtained from the photon energy dependency of the absorption coefficient described as [27].

$$(ah\nu) = A(h\nu - E_g)^p, \quad (4)$$

where  $A$  is a constant depending on the transition probability. The  $p$  is an index and equal to 2 and 1/2 for indirect and direct transitions, respectively. Analysis of the experimental data revealed that  $(ah\nu)$  and  $(h\nu - E_g)$  relation gives a good coherence for  $p = 1/2$  corresponding to direct band gap transitions. The direct band gap energy was found from the analysis of ellipsometry data as 1.53 eV which shows a good consistency with previously reported value of 1.51 eV obtained from the absorption measurements [13].

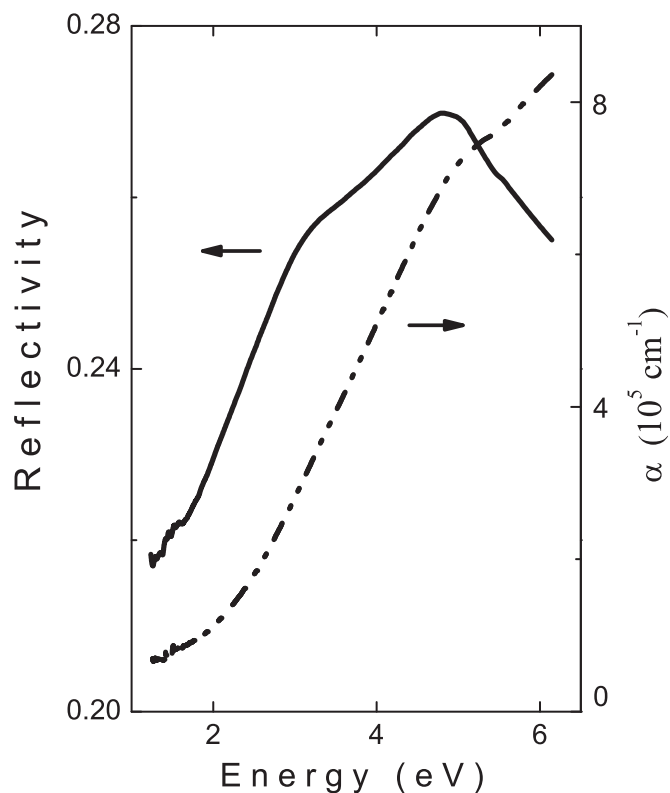


Fig. 5. Spectral dependencies of the reflectivity and absorption coefficient of  $\text{CuIn}_5\text{S}_8$  calculated from ellipsometry data.

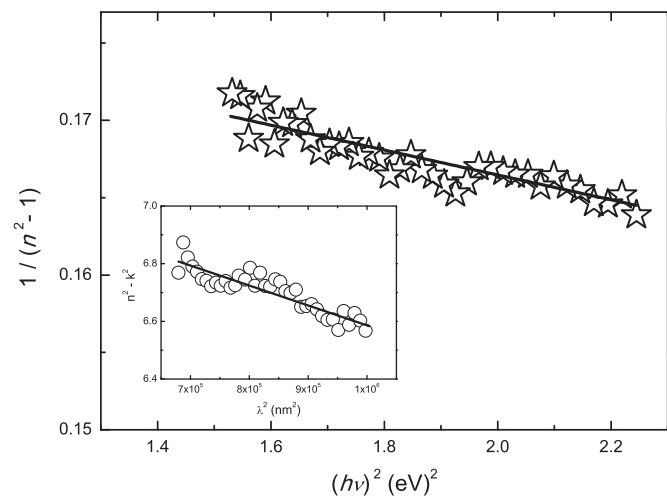


Fig. 6. The plot of  $(n^2 - 1)^{-1}$  vs.  $(h\nu)^2$  in the  $h\nu < E_g$  range. Stars are experimental data and solid line represents the linear fit. Inset: Plot of  $\epsilon_1$  vs.  $\lambda^2$ . Circles are experimental data and solid line shows the linear fit.

The photon energy dependence of pseudorefractive index can be analyzed in the below band gap region ( $h\nu < E_g$ ) using Wemple and DiDomenico single-effective-oscillator model in which  $n$  and  $h\nu$  are related by [28].

$$n^2(h\nu) = 1 + \frac{E_{so}E_d}{E_{so}^2 - (h\nu)^2} \quad (5)$$

where  $E_{so}$  and  $E_d$  represents the single oscillator energy and dispersion energy, respectively. The parameter  $E_d$  is a measure of the strength of the inter-band optical transition. Wemple and DiDomenico have related this parameter to the coordination number

for anion and the valence electron number per anion. The parameter  $E_{so}$  is an average energy band gap. The values of  $E_d = 26.1$  eV and  $E_{so} = 4.76$  eV were obtained from the intercept and the slope resulting from the extrapolation of the curve of Fig. 6, representing the plots of  $(n^2 - 1)^{-1}$  versus  $(h\nu)^2$ . The zero-frequency refractive index ( $n_0$ ) and dielectric constant ( $\epsilon_0$ ) were also calculated as  $n_0 = 2.55$  and  $\epsilon_0 = n_0^2 = 6.50$ .

Spitzer–Fan model gives real component of the pseudodielectric function as [29].

$$\epsilon_1 = n^2 - k^2 = \epsilon_\infty - \left[ \frac{e^2}{\pi c^2} \right] \left( \frac{N}{m^*} \right) \lambda^2 \quad (6)$$

where  $\epsilon_\infty$  is the high-frequency dielectric constant in the absence of any contribution from free carriers,  $N$  is the carrier concentration,  $m^*$  is the effective mass,  $c$  is the speed of light and  $e$  is the electronic charge. Inset of Fig. 6 presents the  $\epsilon_1$  vs.  $\lambda^2$  to find  $\epsilon_\infty$  and  $N/m^*$  from the intersection of plot with  $\epsilon_1$ -axis and slope of the linear fit, respectively.  $\epsilon_\infty$  and  $N/m^*$  values were obtained as 7.3 and  $8.5 \times 10^{47} \text{ g}^{-1} \text{ cm}^{-3}$ , respectively. The values of high-frequency dielectric constant reported in Ref. [9] for  $\text{CuIn}_5\text{S}_8$  thin films varied between 8.88 and 16.78 for substrate temperatures from 30 to 200 °C.

#### 4. Conclusions

Optical properties of  $\text{CuIn}_5\text{S}_8$  crystals were investigated by ellipsometry measurements. Spectral dependence of components of pseudodielectric function, pseudorefractive index, pseudoe extinction coefficient, reflectivity and absorption coefficients were established from the analysis of ellipsometry experiments carried out in the 1.2–6.2 eV range using air/sample optical model. The analysis of the absorption data showed the existence of direct transitions in the crystal with energy band gap of 1.53 eV. Oscillator parameters; single effective dispersion oscillator energy, dispersion energy, zero-frequency refractive index and dielectric constant were determined using single-effective-oscillator model suggested by Wemple and DiDomenico. Spitzer–Fan model was also applied to find the high-frequency dielectric constant and the ratio of carrier concentration to effective mass.

#### References

- [1] L. Gastaldi, L. Scaramuzza, *Acta Crystallogr. B* 35 (1979) 2283.
- [2] M. Gannouni, M. Kanzari, *J. Alloy. Compd.* 509 (2011) 6004.
- [3] M. Gannouni, M. Kanzari, *Appl. Surf. Sci.* 257 (2011) 10338.
- [4] I.V. Bodnar, *Semiconductors* 46 (2012) 602.
- [5] I.V. Bodnar, E.A. Kudritskaya, I.K. Polushina, V.Yu Rud, Yu.V. Rud, *Semiconductors* 32 (1998) 933.
- [6] M. Gannouni, I. Ben Assaker, R. Chtourou, *Mater. Res. Bull.* 61 (2015) 519.
- [7] N. Khedmi, M. Ben Rabeh, M. Kanzari, *Energy Procedia* 44 (2014) 61.
- [8] A. Sinaoui, F. Chaffar-Akkari, B. Gallas, D. Demaille, M. Kanzari, *Thin Solid Films* 590 (2015) 111.
- [9] N. Hemiri, M. Kanzari, *Solid State Commun.* 160 (2013) 32.
- [10] M. Gannouni, I. Ben Assaker, R.J. Chtourou, *J. Electrochem. Soc.* 160 (2013) H446.
- [11] L. Makhova, R. Szargan, I. Kononov, *Thin Solid Films* 472 (2005) 157.
- [12] L. Makhova, I. Kononov, *Thin Solid Films* 515 (2007) 5938.
- [13] N.S. Orlova, I.V. Bodnar, E.A. Kudritskaya, *Cryst. Res. Technol.* 33 (1998) 37.
- [14] N.M. Gasanly, A.Z. Magomedov, N.N. Melnik, *Phys. Status Solidi B* 117 (1993) K31.
- [15] H. Neumann, H. Sobotta, V. Riede, V.E. Tezlevan, N.N. Syrбу, *Cryst. Res. Technol.* 25 (1990) 579.
- [16] I.V. Bodnar, A.G. Karoza, B.V. Korzun, G.F. Smirnova, *Inorg. Mater.* 37 (1981) 152.
- [17] N.M. Gasanly, *Pramana* (in press).
- [18] JCPDS (Joint Committee on Powder Diffraction Standart) Card no: 24-0361.
- [19] C. Paorici, L. Zanotti, L. Gastaldi, *Mater. Res. Bull.* 14 (1979) 469.
- [20] M. Robbins, M.A. Miksovsky, *Mater. Res. Bull.* 6 (1971) 359.
- [21] H. Fujiwara, *Spectroscopic Ellipsometry Principles and Applications*, John Wiley & Sons, New York, 2007.

- [22] S.G. Choi, D.H. Levi, C. Martinez-Tomas, V.M. Sanjose, J. Appl. Phys. 106 (2009) 053517.
- [23] T.J. Kim, J.J. Yoon, S.Y. Hwang, D.E. Aspnes, Y.D. Kim, H.J. Kim, Y.C. Chang, J. D. Song, Appl. Phys. Lett. 95 (2009) 111902.
- [24] M.R. Buckley, F.C. Peiris, O. Maksimov, M. Munoz, M.C. Tamargo, Appl. Phys. Lett. 81 (2002) 5156.
- [25] L. Duran, J. Castro, J. Naranjo, J.R. Fermin, C.A. Durante Rincon, Mater. Chem. Phys. 114 (2009) 73.
- [26] M.I. Alonso, M. Garriga, C.A. Durante Rincon, M. Leon, Appl. Phys. Lett. 88 (2000) 5796.
- [27] J.I. Pankove, Optical Processes in Semiconductors, Prentice Hall, New Jersey, 1971.
- [28] S.H. Wemple, M. Di Domenico, Phys. Rev. B 143 (1971) 1338.
- [29] W.G. Spitzer, H.Y. Fan, Phys. Rev. 106 (1957) 882.